

JLAB12 Activity report 2025

M. Mirazita (Resp.), N. Nicholson (visiting from Duquesne University, USA),
G. Pecar (INFN-DOE Summer student exchange program), P. Rossi, S. Tomassini

1 Introduction

The JLAB12 group of LNF participates in the physics program carried on by the CLAS collaboration in the Hall B of the Jefferson Laboratory (JLab). The LNF group is involved in the data taking and analysis of the CLAS experiment and in the operation of the two modules of the Ring Imaging Cherenkov (RICH) detector of the CLAS12 spectrometer, that was completed in 2022. In addition, the group is also involved in the design of the target cryostat and of the recoil detector for the future transversely polarized target data taking.

2 CLAS data taking

During 2025, the *Run Group L* experiment took data in the Hall B of the JLab. This experiment included several partonic structure measurements, such as the Deeply Virtual Compton Scattering (DVCS), the Deeply Virtual meson production and the EMC effect, on light nuclei. The core of the experiment is the ALERT detector, a gaseous hydrogen, deuterium or He⁴ target equipped with a drift chamber and a time-of-flight detector for the measurement of recoil particles.

3 CLAS data analysis

The LNF group is involved in several analyses with both unpolarized and longitudinally polarized target aiming at studying the nucleon structure through semi-inclusive electroproduction measurements in the Deeply Virtual Scattering region.

A collaboration with the Duquesne University (USA) has been started in 2025 with the goal of measuring the Beam Spin Asymmetry (BSA) in the electroproduction of a proton and K⁺ pair on an unpolarized hydrogen target, with the kaon produced in the forward direction and the proton in the backward direction. This measurement gives access to the Fracture Functions, partonic distribution functions that describe the conditional probability to produce a hadron from the fragmentation of the quark struck by the virtual photon and a second hadron from the fragmentation of the target.

The analysis has been started and carried out by N. Nicholson, a student of the Duquesne University who visited LNF during summer 2025, and used data of the *Run Group A* experiment collected in 2018 and 2019. The forward scattered kaon can be either identified by the forward time-of-flight (FTOF) or by the RICH detector of CLAS12. In the first case, one obtains high statistics, since the FTOF covers the 6 azimuthal sectors of CLAS12, but limited π/K separation power and therefore limited kinematic coverage at high momentum. In the second case, one obtains lower statistics, since the RICH covers only one sector in the data under analysis, but high π/K separation power and full kinematic coverage. In Fig. 1 we show the missing mass of the reaction $ep \rightarrow e'K^+pX$ for the 2018 (red histogram) and 2019 (blue histogram) data sets. Here, kaons are

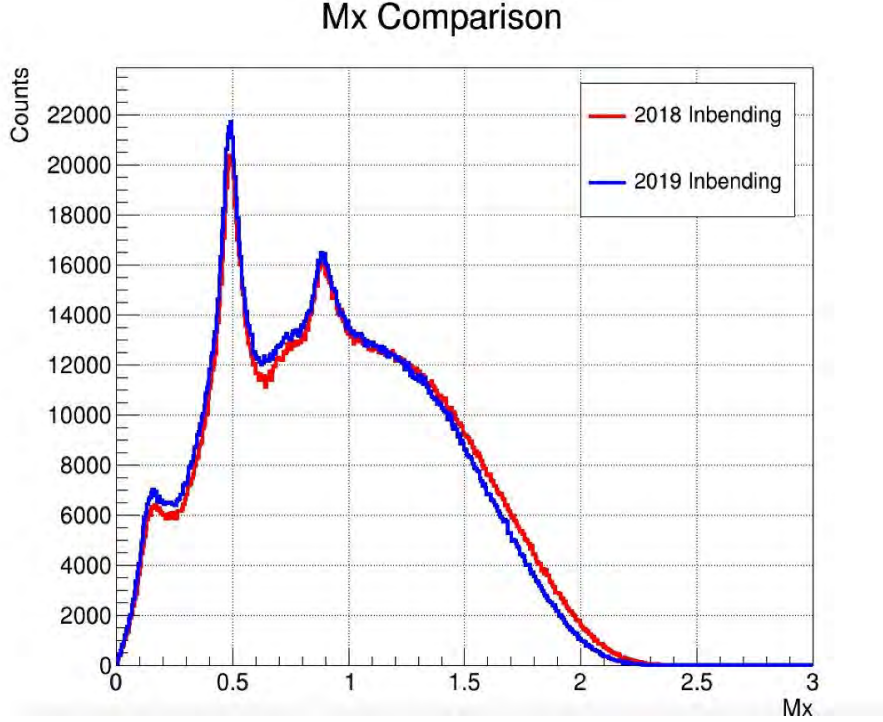


Figure 1: *Missing mass of the reaction $ep \rightarrow e'K^+pX$ for the data taken in 2018 (red histogram) and 2019 (blue histogram).*

selected using the FTOF with the cut $P < 3$ GeV/c. The three peaks visible in the distributions correspond to exclusive reactions, namely:

- $ep \rightarrow e'K^+\Lambda$, with the subsequent weak decay $\Lambda \rightarrow p\pi^-$, the pion being undetected;
- $ep \rightarrow e'K^+K^-$, with the negative kaon undetected;
- $ep \rightarrow e'K^+K^*(890)^-$, with the negative K^* undetected.

In order to properly select the region of validity of the Fracture Function formalism, a cut $M_x > 1$ GeV has been applied to remove the exclusive channels. The next step in the analysis will be the optimization of the cuts to select kaons in the RICH detector and then the calculation of the BSA, defined, up to kinematic prefactors, as

$$BSA \approx \frac{N^+ - N^-}{N^+ + N^-} \quad (1)$$

where N^+ and N^- are the number of events produced with positive and negative electron beam helicity.

4 The RICH detector

The CLAS12 RICH detector has been built with the goal of obtaining clean separation of charged kaons from pions and protons in the momentum range from 3 to 8 GeV/c. It is composed of two

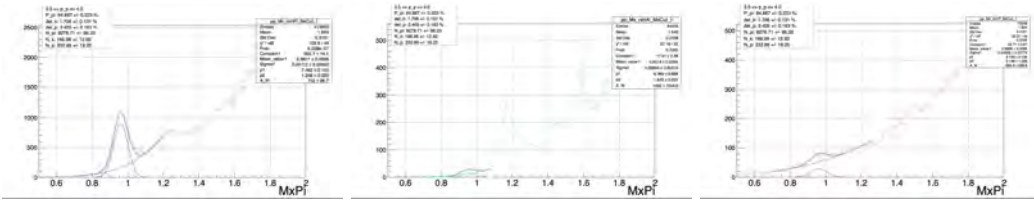


Figure 2: *Missing mass distributions of $e'\pi^+X$ (left), $e'K^+X$ (center) and $e'pX$ (right) events.*

modules, installed in opposite azimuthal sectors of CLAS12, with an aerogel radiator, an array of multianode photomultiplier tubes (MAPMTs) for the Cherenkov light detection and a mirror system.

The radiator is composed of 102 tiles assembled in two sections: the forward angle one made by one layer with 2 cm thickness and the large angle one made by two layers with 3 cm thickness each. The mirror system is composed of 10 carbon fiber spherical mirrors and 7 glass planar mirrors, for a total surface of about 10 m². The photodetector array uses 391 MAPMT Hamamatsu H12700 and H8500, each composed of a matrix of 8×8 matrix of pixel with about 6 mm pixel size, for a total of 25024 independent readout channels per module. The readout electronics is based on the MAROC3 chip, a 64 channel microcircuit dedicated to MAPMT pulse processing. The MAROC3 is configured and read out by a FPGA optically linked with the data acquisition node.

4.1 RICH performance studies

Basic quantities to quantify the performance of a PID detector are the purity, i.e. the fraction of identified hadrons with correct ID, and the contamination, i.e. the fraction of identified hadrons with wrong ID. We started by evaluating these quantities for the π^+ , because of the higher statistics and relatively straightforward method that can be used. This task has been pursued by G. Pecar during his LNF visit under the INFN-DOE Summer Student exchange program. We selected $ep \rightarrow e'h^+X$ events, where $h^+ = \pi^+, K^+, p$ is a charged hadron identified in the RICH. In order to have sufficiently reliable PID, at least three Cherenkov photons per track are required. For each hadron ID, we plot the missing mass in the region around 1 GeV, corresponding to the nucleon mass and fit it with a function composed of a gaussian and a smooth background. It is clear that the $N(e\pi^+n)$ events in the nucleon peak in the $ep \rightarrow e'\pi^+X$ corresponds to correctly identified pions, while the $N(eK^+n)$ ($N(epn)$) events in the $ep \rightarrow e'K^+X$ ($ep \rightarrow e'pX$) events corresponds to wrongly identified pions. We define as purity as:

$$P_{\pi^+} = \frac{N(e\pi^+n)}{N(e\pi^+n) + N(eK^+n) + N(epn)} \quad (2)$$

where the number of events in the nucleon peak are estimated either from the integral of the gaussian curve or by subtracting the integral of the background to the total number of events in the 3σ interval around the peak position. Examples of the missing mass distributions and of the fits are shown in Fig. 2.

In the Fig. 3, we show the purity of the π^+ identification as a function of the momentum. It is around 95% over the entire momentum range with a very small decrease toward the highest values.

4.2 RICH alignment

The RICH particle identification (PID) software uses a likelihood approach that compares the measured arrival time and reconstructed Cherenkov angle of the photon hits on the MAPMT plane

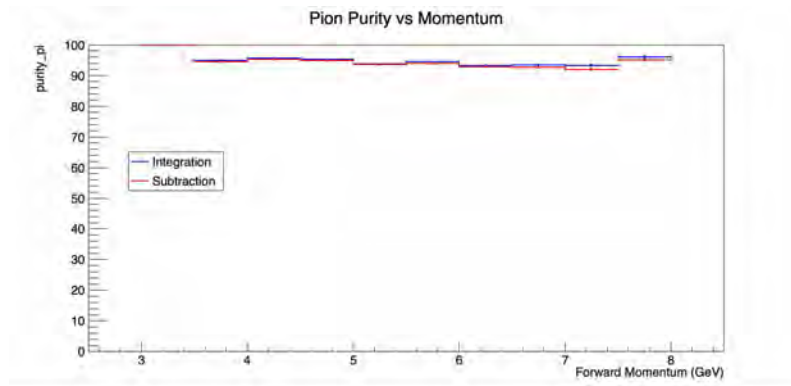


Figure 3: *Positive charged pion purity as a function of the momentum from the RICH PID.*

with the expected ones, calculated from the path of the charged tracks that crossed the aerogel radiator and the path of the photons inside the RICH. A crucial ingredient of this approach is the precise knowledge of the position of the RICH with respect to the CLAS12 tracking system and of the active elements (radiator, mirrors, MAPMT) inside the RICH. It is a complicated task, since at least 66 alignment parameters, highly correlated, must be precisely determined for each module. Reliable results have been obtained so far only for the more forward angles, where a large fraction of the photons is detected with no reflections on the mirror.

A major achievement of 2025 has been the development, in collaboration with the Duke University (USA), of a new alignment protocol that allowed for the first time to extend the particle identification capabilities of the detector in its full kinematic coverage. This alignment protocol is based on a Bayesian Optimization approach that utilizes the TuRBO software ¹⁾, specifically designed to study high dimensional problems. The software performs an initial survey of the multi-dimensional parameter space, defines a trust region centered around the best solution found so far and then tries successive improvements in the trust region.

A special care has been devoted to the construction of the objective function of the alignment. It requires, regardless of how many reflections they have had, same average Cherenkov angle for all the photons ¹ and minimal RMS.

As an example of the results, in Fig. 4 we show the Cherenkov angle distributions for π^- crossing one aerogel tile in the upper section of the radiator plane and photons detected after two reflections, the first one on a spherical mirror and the second one on one of the two frontal planar mirrors. The left plot shows the distributions before the alignment, where each different mirror has a different peak position, different width and even a two peak structure. The right plot shows the same distributions after the alignment, where all the mirrors have same peak position and same width. It is worth noting that the alignment procedure used so far was never able to provide satisfactory results for the photons generated in the second section of the radiator.

In Fig. 5 we show the kinematic coverage, polar angle versus momentum, for negative (left) and positive (right) pions identified in the RICH, after the alignment has been completed. The band of lower efficiency correspond to the dead areas between the radiator planes. These plots have been produced from data taken with torus field with negative polarity, similar results are obtained by switching both torus polarity and pion charge.

Studies are in progress to investigate the systematic uncertainties on the estimation of the

¹For photons that, due to multiple reflections, passed two times through the aerogel radiator, a negative shift of 2 mrad has been imposed, as shown by the simulations.

Layer 203, Tile 7 — nominal vs aligned

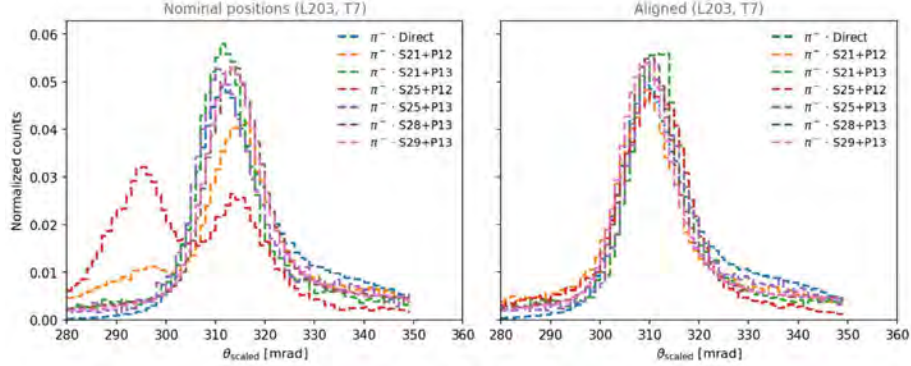


Figure 4: Cherenkov angle distributions for π^- crossing one aerogel tile and detected after two reflections before (left) and after (right) the alignment. The first reflection is on a spherical mirror (labeled as S21 to S29) and one frontal planar mirror (labeled as P12 or P13).

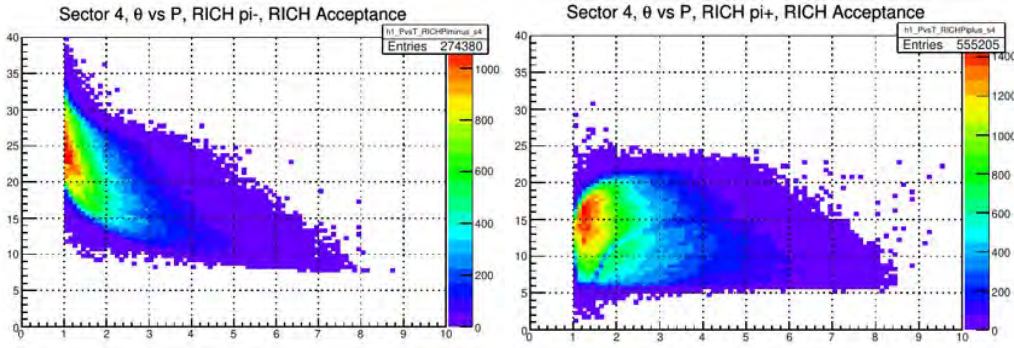


Figure 5: Kinematic coverage, polar angle versus momentum, for π^- (left plot) and π^+ (right plot) identified in the RICH.

alignment parameters. Tools are also being developed in order to implement a suite that allows the users to automatically perform the alignment of the RICH of all the CLAS12 data collected.

5 Transversely polarized target

The *Run Group H* is dedicated to the data taking with a transversely polarized target and includes three experiments: the study of the SIDIS reactions with one or two hadrons in the final state and the DVCS measurement. The three experiments were originally submitted assuming a frozen spin *HD* target and have been approved with high rating under the condition that the *HD* target could be operated with a high energy electron beam. The tests performed showed that the heat produced by the beam significantly reduces the depolarization time to a level that is not manageable in normal experimental condition. Therefore the run group decided to switch to a conventional dynamically polarized NH_3 target. The proposal with the new target configuration has been reviewed by the Program Advisory Committee of JLab in July 2025 and approved confirming the high scientific rate of the original proposal.

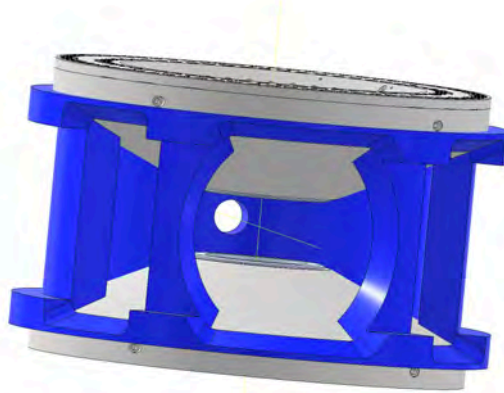


Figure 6: *The new design of the cryostat of the transversely polarized target, showed in blue.*

The large cryostat of the ammonia target has been found not compatible with the CLAS12 central detector, that will be removed and replaced by a new recoil detector, specifically designed to detect low energy protons in the DVCS experiment. The LNF group is responsible for the design of the cryostat of the polarized target and of the recoil detector.

The design of the target is based on the existing target used in Hall A and C of JLab. However, this target doesn't match the acceptance of the CLAS12 forward detector and of the large angle recoil detector. Therefore, a revision of the design of the target cryostat has been performed, to allow larger windows in the forward and lateral directions while still keeping the deformations due to the magnetic forces generated by the 5 T field within the uniformity requirements. The new, still preliminary, design is shown in Fig. 6.

The new recoil detector covers the large polar angles between about 40° and 70° with an azimuthal aperture of about $\pm 25^\circ$. It is composed of three tracking stages of μ Rwell with maximum dimensions of 500×1000 cm² and one TOF array, made by plastic scintillators bars read out by SiPM. The current design of the detector is shown in Fig. 7.

6 Workshop organization

From December 15 to 19, we organized at the LNF the workshop *Strangeness in Hard Processes 2025* ²⁾, chaired by M. Mirazita and P. Rossi. The goal of the workshop was to bring together leading theorists and experimentalists to explore the multifaceted role of strangeness, embodied in kaons and other strange hadrons, in hard QCD processes. The main topics of the workshop have been:

- Kaon Production Mechanisms
- Kaon Structure and Distribution Functions
- Transverse Momentum Distributions (TMDs)

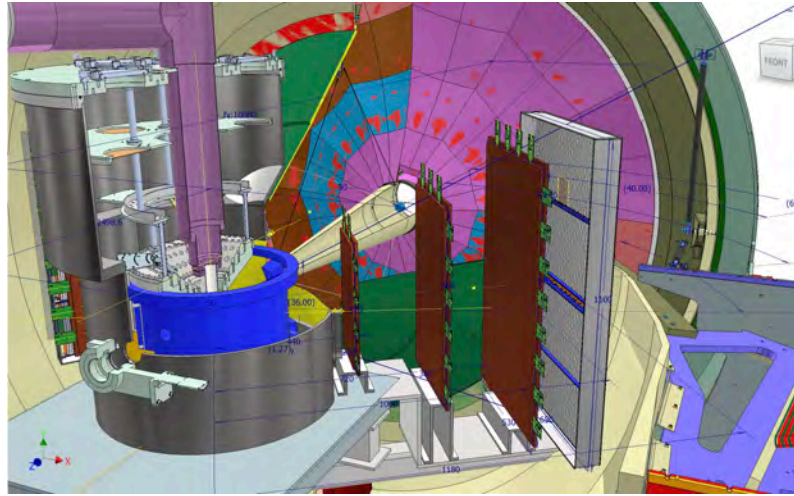


Figure 7: *Drawing of the recoil detector in the target region.*

- Hadronization and Fragmentation Dynamics
- Theoretical Approaches and Models
- Experimental Facilities and Techniques
- Phenomenology and Data-Theory Interface

The participation, part in person and part remote, to the workshop was only for invited speakers, with a total of 29 contributions.

References

1. arXiv:1910.01739
2. <https://indico.cern.ch/event/1588046/>